APPLIED MICROBIAL AND CELL PHYSIOLOGY

PEP3 overexpression shortens lag phase but does not alter growth rate in *Saccharomyces cerevisiae* exposed to acetic acid stress

Jun Ding[1,2] · Garrett Holzwarth[2,3] ·
C. Samuel Bradford[4] · Ben Cooley[5] ·
Allen S. Yoshinaga[2,3] · Jana Patton-Vogt[5] ·
Hagai Abeliovich[6] · Michael H. Penner[2] ·
Alan T. Bakalinsky[1,2,3]

Abstract In fungi, two recognized mechanisms contribute to pH homeostasis: the plasma membrane proton-pumping ATPase that exports excess protons and the vacuolar proton-pumping ATPase (V-ATPase) that mediates vacuolar proton uptake. Here, we report that overexpression of *PEP3* which encodes a component of the HOPS and CORVET complexes involved in vacuolar biogenesis, shortened lag phase in *Saccharomyces cerevisiae* exposed to acetic acid stress. By confocal microscopy, *PEP3*-overexpressing cells stained with the vacuolar membrane-specific dye, FM4-64 had more fragmented vacuoles than the wild-type control. The stained overexpression mutant was also found to exhibit about 3.6-fold more FM4-64 fluorescence than the wild-type control as determined by flow cytometry. While the vacuolar pH of the wild-type strain grown in the presence of 80 mM acetic acid was significantly higher than in the absence of added acid, no significant difference was observed in vacuolar pH of the overexpression strain grown either in the presence or absence of 80 mM acetic acid. Based on an indirect growth assay, the *PEP3*-overexpression strain exhibited higher V-ATPase activity. We hypothesize that *PEP3* overexpression provides protection from acid stress by increasing vacuolar surface area and V-ATPase activity and, hence, proton-sequestering capacity.

Keywords *Saccharomyces cerevisiae* · Yeast · Acetic acid · *PEP3* · V-ATPase · HOPS · CORVET · Vacuole · *STM1* · *PEP5*

✉ Alan T. Bakalinsky
alan.bakalinsky@oregonstate.edu

1   Department of Biochemistry and Biophysics, Oregon State University, Corvallis, OR, USA

2   Department of Food Science and Technology, Oregon State University, Corvallis, OR, USA

3   Department of Microbiology, Oregon State University, Corvallis, OR, USA

4   Department of Environmental & Molecular Toxicology, Oregon State University, Corvallis, OR, USA

5   Biological Sciences, Duquesne University, Pittsburgh, PA, USA

6   Department of Biochemistry and Food Science, Hebrew University, Rehovot, Israel

Introduction

While acetic acid is a normal by-product of yeast fermentation, high concentrations can inhibit growth. Current interest in increasing the acetic acid tolerance of industrial strains of *Saccharomyces cerevisiae* is motivated in part by efforts to develop lignocellulosic biomass as a renewable biofuel because acetic acid is an undesirable yet unavoidable byproduct of the pre-fermentation processing of lignocellulose (Palmqvist and Hahn-Hägerdal 2000). Exogenous acetic acid is taken up by *S. cerevisiae* in undissociated form by passive diffusion or through the Fps1 channel (Mollapour and Piper 2007). It dissociates in the neutral environment of the cytosol, generating acetate anions and protons that acidify the cytoplasm. Yeast cells rely to a significant, but not exclusive extent, on the activity of the proton-pumping plasma membrane ATPase, Pma1, to extrude

protons at the expense of ATP (Eraso and Gancedo 1987). Under normal physiologic conditions, the vacuolar proton-pumping ATPase (V-ATPase) also contributes to pH homeostasis as the acidic vacuole is a proton sink (Li and Kane 2009; Schumacher and Krebs 2010).

The vacuole itself is a dynamic organelle whose biogenesis and fragmentation depend on vesicle-vesicle/vesicle-vacuole fusion and fission events, respectively, that occur during growth and in response to environmental signals (Li and Kane 2009; Weisman 2003). Genetic screens have identified many of the genes involved in vacuolar biogenesis in yeast, including those encoding SNARE proteins (Nichols et al. 1997; Wickner 2010), the V-ATPase (Coonrod et al. 2013), and proteins found in the HOPS and CORVET complexes that participate in tethering transport vesicles to the vacuole or to other endocytic compartments (Nakamura et al. 1997; Price et al. 2000; Peplowska et al. 2007; Balderhaar and Ungermann 2013). Loss of any of the genes encoding proteins in these two complexes results in vacuolar defects, while loss of 3 of the 4 so-called class C core genes that encode proteins shared by both complexes: Vps11 (Pep5), Vps16, Vps18 (Pep3), but not Vps33 (Balderhaar and Ungermann 2013), has been reported to drastically increase sensitivity to acetic acid (Kawahata et al. 2006). Although overexpression of *PEP3* (Arlt et al. 2011), *VAM6* (a member of HOPS complex, Harding et al. 1995) or *VPS3* (a member of CORVET complex, Peplowska et al. 2007) has previously been reported to result in more fragmented vacuoles, to our knowledge, the present study is the first to document an associated decrease in lag phase in acetic acid-stressed cells.

Because of limitations inherent in the widely used *S. cerevisiae* gene deletion libraries that restrict the extent of acetic acid resistance that can be obtained in the multiply auxotrophic library mutants (Ding et al. 2013), we sought acetic acid-resistant mutants by screening a library of overexpressed yeast genes (Jones et al. 2008). Here, we report that overexpression of *PEP3* increases yeast tolerance for acetic acid by shortening lag phase. Based on an analysis of vacuole morphology and function in the *PEP3*-overexpression mutant, we propose that the shortened lag phase results from an increased capacity to sequester protons.

Materials and methods

Yeast strains, plasmid construction, growth conditions, transformation

Yeast strains and plasmids and PCR primers used in the present study are listed in Tables 1 and S1 in the Supplementary Material, respectively. *PEP3*, *PEP5*, and *STM1* were amplified by PCR from S288c genomic DNA, using the primers listed in Table S1 in the Supplementary Material. The amplified genes were digested with restriction enzymes whose recognition sites had been added to the primers to allow release of the alleles which were then subcloned into appropriately digested pGP564 to yield pGP564-*PEP3*, pGP564-*PEP5*, and pGP564-*STM1*. Strains were grown in YEPD (1 % yeast extract, 2 % peptone, 2 % glucose), YEPD, pH 7.5 (YEPD-7.5), YNB+2 % glu (Bacto yeast nitrogen base without amino acids containing 2 % glucose), YNB-4.8+2 % glu (YNB, pH 4.8+2 % glucose), or YEPG-5 (1 % yeast extract, 2 % peptone, 2 % glycerol, pH 5). Agar-based media were sterilized by autoclaving. Liquid media were sterilized by filtration through a 0.45 μ membrane. If pH was adjusted or supplements were added, final medium pH and supplements are indicated. A 2 N stock of acetic acid, pH 4.8 was prepared monthly. To determine vacuolar pH, cells were grown in synthetic complete medium using homemade low-fluorescence yeast nitrogen base lacking riboflavin and folic acid to minimize autofluorescence: 5 g/l $(NH_4)_2SO_4$, 1 g/l KH_2PO_4, 0.5 g/l $MgSO_4$, 0.1 g/l NaCl, 0.1 g/l $CaCl_2$, 0.5 mg/l H_3BO_3, 0.04 mg/l $CuSO_4$, 0.1 mg/l KI, 0.2 mg/l $FeCl_3$, 0.4 mg/l $MnSO_4$, 0.2 mg/l Na_2MoO_4, 0.4 mg/l $ZnSO_4$, 2 μg/l biotin, 0.4 mg/l calcium pantothenate, 2 mg/l inositol, 0.4 mg/l niacin, 0.2 mg/l para-aminobenzoic acid, 0.4 mg/l pyridoxine HCl, 0.4 mg/l thiamine supplemented with 2 % glucose in the presence or absence of 80 mM acetic acid, pH 4.8. All chemicals for the homemade medium were from Sigma-Aldrich (St. Louis, MO, USA). *S. cerevisiae* S288c *leu2Δ* was transformed with pGP564 (control), pGP564-*PEP3*, pGP564-*PEP5*, or pGP564-*STM1* using standard procedures (Gietz et al. 1995). Transformants were selected on YNB+2 % glu plates and verified by diagnostic PCR.

Screening of yeast overexpression library for acetic acid-resistant mutants

S288c *leu2Δ* was transformed with a yeast tiling library consisting of 1588 pGP564-based plasmids containing 4–5 yeast ORFs on average, which covers 97 and 95 % of the yeast genome at the physical and functional levels, respectively (Jones et al. 2008; YSC4613, Thermo Scientific, Waltham, MA, USA). Overexpression is based on use of pGP564, a high-copy number, *LEU2* plasmid containing 2 μ sequences. A DNA pool containing the library was generated by replicating the original ~1600 *Escherichia coli* clones harboring the plasmids to 96-well plates containing LB+50 μg/ml kanamycin, allowing clones to grow individually overnight at 37 °C, pooling the clones, and extracting total plasmid DNA (Qiagen Sci. Inc., Germantown, MD, USA). S288c *leu2Δ* was then transformed with the pooled plasmids and transformants were selected on YNB+2 % glu. A total of 4491 independent Leu[+] yeast transformants were obtained, pooled, and stored at −70 °C. Liquid YNB+2 % glu containing 140 mM acetic acid

Table 1 Plasmids and yeast strains used in this study

Plasmids	Features	Source
pGP564	Leu$^+$, Kan^r, 2 μ	YSC4613, Thermo Scientific, Waltham, MA, USA
pGP564-YGM18p06	pGP564-*SPE4*[a], *SMD3*, *PEP3*, YLR149C, YLR149C-A, *STM1*, *PCD1*[b], YLR152C[c]	YSC4613, Thermo Scientific, Waltham, MA, USA
pGP564-*PEP3*	pGP564-*PEP3*	This study
pGP564-*PEP5*	pGP564-*PEP5*	This study
pGP564-*STM1*	pGP564-*STM1*	This study
Strains	Genotype	Source
S288c	*MATα SUC2 mal mel gal2 CUP1*	ATCC 204508, Manassas, VA, USA
S288c *leu2Δ*	*MATα SUC gal mal mel flo1 flo8-1 hap bio1 bio6 leu2Δ::KanMX*	Ding et al. 2013
S288c *leu2Δ*/pGP564	*MATα SUC gal mal mel flo1 flo8-1 hap bio1 bio6 leu2Δ::KanMX/ pGP564*	This study
S288c *leu2Δ*/pGP564-*PEP3*	*MATα SUC gal mal mel flo1 flo8-1 hap bio1 bio6 leu2Δ::KanMX/ pGP564-PEP3*	This study
S288c *leu2Δ*/pGP564-*PEP5*	*MATα SUC gal mal mel flo1 flo8-1 hap bio1 bio6 leu2Δ::KanMX/ pGP564-PEP5*	This study
S288c *leu2Δ*/pGP564-*STM1*	*MATα SUC gal mal mel flo1 flo8-1 hap bio1 bio6 leu2Δ::KanMX/ pGP564-STM1*	This study
S288c *leu2Δ*/pGP564-YGM18p06	*MATα SUC gal mal mel flo1 flo8-1 hap bio1 bio6 leu2Δ::KanMX/ pGP564-1004*	This study

[a] The 3′ end of the gene is missing (Jones et al. 2008)

[b] The ORF is intact, but might be missing necessary upstream or downstream sequences to be correctly regulated (Jones et al. 2008)

[c] The 5′ end of the gene is missing (Jones et al. 2008)

at pH 4.8 was inoculated with 2×10^5 cfu/ml of cells from the pool of yeast transformants and grown at 30 °C and 200 rpm. After 48 h of growth, diluted aliquots were plated onto YNB+ 2 % glu plates containing either 160 or 180 mM acetic acid at pH 4.8. After 72 h of growth, cells from isolated colonies were re-tested by inoculating fresh aliquots of liquid YNB+2 % glu containing the original 160 or 180 mM acetic acid at pH 4.8. Presumptive acetic acid-resistant mutants that grew upon retesting in the liquid cultures were replica-plated to YNB+ 2 % glu for further analysis.

Identification of plasmids and genes

Plasmids in the presumptive acetic acid-resistant mutants were extracted using a phenol-chloroform-isopropanol method (Sobanski and Dickinson 1995). The ends of the yeast contigs in the plasmids were sequenced by PCR at the Oregon State University Center for Genome Research and Biocomputing using a pair of flanking primers (M13 and M48; Table S1 in the Supplementary Material) specific to pGP564. Candidate ORFs identified in the end sequences by searching the *Saccharomyces* Genome Database (http://www.yeastgenome. org) provided sufficient information to identify the original tiling plasmids. The tiling library database was consulted to determine the precise contig and associated ORFs. Individual ORFs were then prioritized based on whether the genes were

known to be intact within the contig and could plausibly confer resistance on the basis of known function. In order to avoid potential complications arising from second-site mutations in the original clones subjected to prolonged selection in the presence of elevated acetic acid concentrations, all subsequent analyses were performed on S288c *leu2Δ* newly transformed with individual contigs obtained from the original tiling library or candidate genes cloned independently from S288c and ligated into pGP564.

Determination of growth rate and lag phase duration

Growth rates and duration of lag phase were determined by measuring A_{600} values in aerobic shake flask cultures grown in YNB-4.8+2 % glu (30 ml/250 ml flask) incubated at 30 °C and 200 rpm with or without added acetic acid. The shake flask cultures were inoculated to a starting A_{600} value of 0.1–0.3 using a 24-h inoculum grown in YNB-4.8+2 % glu at 30 °C and 200 rpm. The inoculum was washed twice in sterile distilled water and resuspended in an equal volume of sterile distilled water prior to use. Lag phase was defined as the time that elapsed before exponential growth was detectable by A_{600} measurement and was determined as described (Xu et al. 1994). The growth experiments were performed in triplicate.

Determination of survival

Survival was determined by plating cells following a 1.5-h exposure to 0, 140, and 160 mM acetic acid in aerobic 1 ml YNB-4.8+2 % glucose cultures at 30 °C and 200 rpm ($n=3$). The 1.5-h treatment was chosen to minimize the possibility of growth of the acetic acid-treated cultures which would otherwise confound interpretation of the survival data. Cultures were inoculated to about 2×10^6 cells/ml (equivalent to 0.1–0.2 A_{600} units) using a 24-h inoculum grown in YNB-4.8+2 % glu at 30 °C and 200 rpm that had been washed twice in sterile distilled water and resuspended in an equal volume of sterile distilled water. Initial viability of the inoculum was determined by plating on YNB+2 % glucose plates to yield 50–300 colonies/plate. Following the 1.5-h exposure to acetic acid, cells were placed on ice, diluted as needed in sterile distilled water, and plated on YNB+2 % glucose plates to yield ~50–150 colonies/plate. Colonies were counted after 3 days at 30 °C. All platings were done in triplicate.

Real-time quantitative PCR

Real-time quantitative (RT-qPCR) was performed as described (Ding et al. 2013). Briefly, total RNA from mid log-phase cultures ($A_{600}=0.8$–1) of S288c leu2Δ/pGP564 and S288c leu2Δ/pGP564-PEP3 was isolated using an RNeasy Mini Kit (Qiagen Sci. Inc.) and was then reverse-transcribed using an iScript cDNA Synthesis Kit (Bio-Rad Laboratories, Hercules, CA, USA). The PCR primers used are listed in Table S1 in the Supplementary Material. ACT1 was used as a housekeeping gene. The RT-qPCR was performed in triplicate using iQ SYBR Green Supermix (Bio-Rad Laboratories). All PCR reactions were mixed in 48-well optical plates and cycled in a thermal cycler (Eco QPCR System, Illumina Inc., San Diego, CA, USA). For each gene, samples were amplified by SYBR PCR to obtain standard curves. Gene expression levels were determined by the $2^{-\Delta\Delta C_T}$ method (Pfaffl 2001) based on the ratio of fluorescence signals in PEP3-overexpressing cells to wild-type cells, normalized to ACT1 expression: $ACT1/\text{target}=2^{C_T^{(ACT1)}-C_T^{(target)}}$ (2006 Real-Time PCR Applications Guide, Bio-Rad Laboratories, Inc.).

Cell size and granularity analysis

Mid-log phase cultures of S288c leu2Δ/pGP564 and S288c leu2Δ/pGP564-PEP3 were collected and sonicated gently for 10 s (model 60 Sonic Dismembrator, Fisher Scientific, Hampton, NH, USA) to disperse cell aggregates. Forward scatter (a relative index of cell size) and side scatter (a relative index of granularity—an indication of organelle content) of incident blue (488 nm) laser light were determined for 200,000 cells/strain on a Beckman Coulter FC 500 cytometer (Beckman Coulter, Pasadena, CA, USA).

Staining of the vacuole with quinacrine

Estimates of vacuolar acidity were determined by quinacrine staining whose fluorescence is inversely proportional to vacuolar pH (Hughes and Gottschling 2012). Briefly, S288c leu2Δ/pGP564 and S288c leu2Δ/pGP564-PEP3 were grown in YEPD with or without 80 mM acetic acid at pH 4.8 and 30 °C to mid-log phase. Approximately 2×10^6 cells were collected and washed once in washing buffer (YEPD, 100 mM HEPES, pH 7.6) and resuspended in 100 μl of the same buffer containing 200 μM quinacrine (Sigma-Aldrich, St. Louis, MO, USA). Cells were incubated for 10 min at 30 °C followed by 5 min on ice. Cells were then harvested by centrifugation and washed twice with ice-cold 100 mM HEPES, pH 7.6, containing 2 % glucose. After centrifugation, the cell pellet was resuspended in the same medium and viewed by fluorescence microscopy (Nikon Eclipse 50i microscope, Tokyo, Japan) within 1 h of staining. Quinacrine fluorescence of 100-μl aliquots of stained cells was quantified in black, 96-well plates (Greiner Bio-One #655076, Frickenhausen, Germany) in a spectrofluorometer (Molecular Devices LLC, Sunnyvale, CA, USA). Fluorescence was normalized to cell number.

FM4-64 labeling of the vacuolar membrane

The vacuolar membrane-specific dye FM4-64 was used to stain the vacuole (Suzuki et al. 2012). Briefly, S288c leu2Δ/pGP564 and S288c leu2Δ/pGP564-PEP3 were grown at 30 °C and 200 rpm in YEPD or YEPD containing 80 mM acetic acid, pH 4.8, to mid-log phase. One-ml samples were collected by centrifugation. The unwashed cell pellets were resuspended in 100 μl of YEPD containing 40 μM N-(3-triethylammoniumpropyl)-4-(ρ-diethylaminophenyl-hexatrienyl) pyridinium dibromide (FM4-64; Invitrogen, Carlsbad, CA, USA) and were incubated for 15 min in the dark at room temperature. Cells were pelleted by centrifugation and washed once with YEPD. After centrifugation, the cell pellet was resuspended in YEPD and incubated for 30 min in the dark at 30 °C. Cells were then pelleted and resuspended in YNB+2 % glu to minimize fluorescence background and photographed using a LSM 510 Meta confocal microscope (Zeiss, Jena, Germany) or were analyzed by flow cytometry (Beckman Coulter FC 500, Pasadena, CA, USA) within 1 h.

Vacuolar surface-to-volume ratio determination

Vacuole size was measured as described (Zieger and Mayer 2012). Cells were grown in YEPD or YEPD containing 80 mM acetic acid, pH 4.8, harvested in mid-log phase and visualized as described for FM4-64 labeling. At least 16 FM4-64 stained vacuoles from cells grown in the absence or

presence of 80 mM acetic acid were analyzed, including multiple vacuoles from individual cells such that all vacuoles within chosen cells were measured. Vacuoles were assumed to be spheres. Their diameters in the xy plane were measured in three different orientations by confocal microscopy using a Zeiss LSM 510 Meta confocal microscope and software. The average diameter based on the three orientations was used in calculations.

Indirect measurement of V-ATPase activity

Because V-ATPase activity is required when yeast grows in YEPD at pH 7.5 (Nelson and Nelson 1990) or on glycerol (YEPG-5) (Ohya et al. 1991), it is possible to estimate V-ATPase activity indirectly by assessing growth under these conditions in the presence vs absence of the V-ATPase-specific inhibitor, concanamycin A. To assay cell growth in YEPD, pH 7.5 (YEPD-7.5) in the presence of concanamycin A, 2×10^5 mid-log phase cells from a YEPD-7.5 overnight culture were collected and diluted into 1 ml of the same medium containing a final concentration of 0.5 % DMSO, with or without 1 μM concanamycin A (Sigma-Aldrich). Cultures were then incubated at 30 °C and 200 rpm. (The DMSO was added because the concanamycin A stock was prepared in DMSO.) Relative growth was calculated by dividing the A_{600} values of concanamycin A-treated cells by A_{600} values of untreated control cells grown in parallel after 24 h. To assay growth in YEPG, pH 5 (YEPG-5) in the presence of concanamycin A, 2×10^5 mid-log phase cells from a YEPG-5 overnight culture were collected and diluted into 200 μl of the same medium containing a final concentration of 0.5 % DMSO with or without 2 μM concanamycin A (Santa Cruz Biotechnology, Dallas, TX, USA) in a 96-well plate. Cultures were incubated at room temperature and 200 rpm. A_{600} readings were measured after 24 h using a spectrofluorometer (Molecular Devices LLC, Sunnyvale, CA, USA). Relative growth was calculated by dividing the A_{600} values of concanamycin A-treated cells by A_{600} values of untreated control cells grown in parallel.

Vacuolar pH

Vacuolar pH was measured essentially as described (Diakov et al. 2013). Briefly, cells were grown overnight at 30 °C at 200 rpm in YNB-4.8+2 % glu in the presence or absence of 80 mM acetic acid. The same medium was inoculated with the overnight culture which was then grown for 4–5 h under the same conditions. About 4×10^6 mid-log phase cells were washed twice and resuspended in the same medium without acetic acid containing 50 μM 2′,7′-bis(2-carboxy-ethyl)-5,6-carboxyfluorescein-acetoxymethyl ester (BCECF-AM; Molecular Probes, Eugene, OR, USA) and incubated for 30 min at 30 °C at 200 rpm. Cells were

collected by centrifugation, washed three times with low-fluorescence yeast nitrogen base without glucose, and resuspended in 100 μl of 1 mM MES pH 5 to determine vacuolar pH by measurement of fluorescence. Fluorescence intensity at 535 nm from excitation at 450 and 490 nm was acquired using a Spectra Max Geminixs multimode microplate reader (Molecular Devices LLC, Sunnyvale, CA, USA). Three biological replicates were performed for acetic acid-free and acetic acid-exposed cells. For each strain tested, a pH standard curve was generated as described (Padilla-López and Pearce 2006) by incubating BCECF-AM-stained cells in calibration buffer containing 50 mM MES, 50 mM HEPES, 50 mM KCl, 50 mM NaCl, 0.2 mM ammonium acetate, 10 mM NaN_3, 10 mM 2-deoxyglucose, 50 μM carbonyl cyanide m-chlorophenylhydrazone, adjusted to five different pH values within the range of 4.5–6.5. The fluorescence intensity ratio of $(535_{emis}/490_{exci})/(535_{emis}/450_{exci})$ was recorded and graphed as a function of the calibration buffer standards to calculate the vacuolar pH of the experimental samples.

Western blotting of V-ATPase subunit Vma2

Western blotting was performed essentially as described (Tal et al. 2007). Briefly, 10 ml of mid-log phase cultures of S288c $leu2\Delta$/pGP564 and S288c $leu2\Delta$/pGP564-PEP3 were pelleted, and the cell pellets were treated with 1 ml of freshly made ice-cold 10 % (w/v) TCA. Following centrifugation and removal of the supernatant, 1 ml of −20 °C acetone was added. The acetone-cell pellet was then disrupted for ~1 min using a probe sonicator (Model 60 Sonic Dismembrator, Fisher Scientific, Waltham, MA, USA). The disrupted pellet was centrifuged again, resuspended in acetone, and sonicated twice more. The cell pellets were then disrupted by vortexing after addition of 100 μl of glass beads (425–600-μm diameter) in 100 μl of cracking buffer (6 M urea, 1 % SDS, 1 mM EDTA, 50 mM Tris-Cl, pH 6.8). An additional 100 μl of cracking buffer were added, and the suspension was mixed and centrifuged at 14,000×g for 5 min. The clarified lysate was transferred to a new tube, and protein levels were determined by the Bradford method (Bradford 1976) using a commercial kit with BSA as standard (Bio-Rad Laboratories, Hercules, CA, USA). About 15 μg of protein per sample were mixed with 2× Laemmli sample buffer, loaded, and separated on an SDS-PAGE gel, and immunoblotted using a semi-dry protein blotting apparatus (Bio-Rad Laboratories, Hercules, CA, USA). After transferring to a nitrocellulose membrane (General Electric Amersham Hybond-C Extra, Fairfield, CT, USA), the proteins were probed with polyclonal antibodies raised against Vma2, a V-ATPase subunit (Life Technologies, Carlsbad, CA, USA) and GADPH (glyceraldehyde-3-P dehydrogenase) which was used as a loading control (Thermo Fisher Scientific, Inc., Waltham, MA, USA). Primary antibodies were

detected using horseradish-peroxidase-conjugated anti-mouse secondary antibody (Life Technologies, Grand Island, NY, USA) followed by enhanced chemiluminescence using the Supersignal West Pico kit (Pierce Biotechnology, Rockford, IL, USA). Visualization of all enhanced chemiluminescence reactions was performed using a ChemiDoc MP imaging system (Bio-Rad Laboratories, Hercules, CA, USA).

Nutrient uptake assays

S288c *leu2Δ*/pGP564 (empty vector control) and S288c *leu2Δ*/pGP564-*PEP3* were pregrown in YNB-4.8+2 % glu overnight to A_{600}=0.7–1.5. The cells were harvested and re-suspended in fresh YNB-4.8+2 % glu (with or without 80 mM acetic acid) to A_{600}=1. Cell suspensions were allowed to equilibrate with shaking for 10 min. For the transport assays, 200 μl aliquots of cells at A_{600}=1 were removed to fresh tubes and placed in a 30° heating block. To start the assay, 50 μl of the indicated radiolabeled nutrient was added to each tube, and transport was allowed to proceed for either 5 or 10 min. A zero time point sample was also taken for each nutrient to determine the extent of non-specific binding of the radiolabel to cells. Ten milliliters of ice-cold water were added to stop the transport reaction, and cells were immediately filtered through glass fiber filters. The filters were washed with 15 ml of water. Radioactivity in the cells was determined by subjecting the filters to liquid scintillation counting (2100TR Packard Liquid Scintillation Analyzer). The concentration of each nutrient in the assay (a labeled and unlabeled mixture) and time of assay were optimized to ensure linear uptake over the given time frame and are as follows: 100 μM ^{3}H-lysine (Perkin-Elmer, Waltham, MA, USA), 5 min; 50 μm ^{3}H-histidine (American Radiolabelled Chemicals, St. Louis, MO, USA), 10 min. Counts per minute were converted to pmoles and normalized to A_{600} values.

Statistical analysis

Statistical significance was assessed using Student's two-tailed paired *t* test (Microsoft Excel, Redmond, WA, USA).

Results

Screening of the overexpression library for acetic acid-resistant mutants

To identify genes whose overexpression could increase acetic acid resistance, a 2 μ-based yeast overexpression library was screened for acetic acid-resistant mutants. An initial selection in YNB+2 % glu containing 140 mM acetic acid (pH 4.8) was chosen because the parental strain (empty vector control) failed to grow or grew poorly at this concentration in

preliminary experiments. This screen resulted in about 50 colonies. Upon re-plating on YNB+2 % glu plates containing either 160 or 180 mM acetic acid (pH 4.8), fewer than 20 of the approximately 50 colonies grew. Retesting the clones in liquid culture containing either 160 or 180 mM acetic acid (pH 4.8) eliminated all but 10 candidates. Sequencing of the inserts from the extracted plasmids revealed 9 different plasmids (Table 2). Three and six clones were isolated from the 160 and 180 mM acetic acid cultures, respectively. Based on the overexpression library database, of the 63 genes found in the 9 clones, the 3′ ends of 6, and the 5′ ends of another 6 were missing. In addition, regulatory sequences may have been missing from 4 other genes. The single clone YGPM18p06 was chosen for further analysis for the following reason. It contained a contig spanning nucleotides 433,497-443,070 of chromosome XII containing *PEP3* whose deletion had previously been shown to result in sensitivity to multiple acids (Kawahata et al. 2006; Lawrence et al. 2004; Schauer et al. 2009; Mira et al. 2010). Only a single clone, YGPM18p06, contained an intact *PEP3* gene in the library.

Acetic acid-stressed *PEP3*-overexpressing cells have shortened lag phase

Table 3 shows growth rates and lag phase duration for S288c *leu2Δ* newly transformed with the individual pGPM18p06 contig, pGP564-*PEP3*, the empty vector pGP564, pGP564-*STM1*, and pGP564-*PEP5* grown in the absence or presence of 140 or 160 mM acetic acid. In all cases, in the absence of acetic acid, the pGPM18p06 clone and *PEP3*-overexpression strain grew about 6 and 15 % faster than the empty vector control, respectively, while lag phase duration for the three strains was the same, about 1.3 h. In the presence of 140 mM acetic acid, the growth rate of the empty vector pGP564 control and *PEP3*-overexpression strains was the same, but about 28 % less than the growth rate of the pGPM18p06 clone. Lag phase duration for the empty vector pGP564 control was about 16.5 h, whereas it was only about 5 and 4 h for the pGPM18p06 clone and *PEP3*-overexpression strain, respectively. At 160 mM acetic acid, the growth rate of the empty vector pGP564 control and *PEP3*-overexpression strains was the same, but was 40 % less than that of the pGPM18p06 clone. Lag phase duration for the empty vector pGP564 control was again about 16.5 h, while it was only about 5 and 6 h for the pGPM18p06 clone and *PEP3*-overexpression strain, respectively. Clearly, *PEP3* overexpression shortened lag phase duration in the presence of acetic acid stress but had no effect on growth rate. As others have pointed out (Swinnen et al. 2014), an increased lag phase observed in cells subjected to a potentially lethal treatment, e.g., acetic acid shock, may reflect a combination of at least two responses: death of a subset of treated cells and a delay in growth of survivors. Because measurement of lag phase by

Table 2 Acetic acid-resistant clones obtained from screening an overexpression library

Clone[a]	Coordinates[b]	Chr[c]	Intact genes	Maximum tested acetic acid tolerance (mM)[d]
YGPM18l24	523739–532483	II	YBP141C, YBR141-W, *MAK5*,	160
YGPM25k02	323339–334823	IV	*BRE1*, YDL073W, *YET3*, YDL071C, *BDF2*, *CBS1*, YDL068W	180
YGPM19a16	166110–176655	VII	*MPT5*, YGL176C, *SAE2*, *BUD13*	180
YGPM3f19	167426–176889	VII	YGL176C, *SAE2*, *BUD13*	180
YGPM11p03	426077–435966	VII	*PNC1*, YGL036W, *MIG1*, YGL034C	160
YGPM6f15	670751–679519	VII	YGP093W, *VAS1*, *RRP46*, *TPC1*, *ASK10*	180
YGPM2m05	33516–41998	IX	YIL165C, *NIT1*, YIL163C, *SUC2*, YIL161W, *POT1*	160
YGPM7m22	556412–575951	X	*YAE1*, *RFC2*, *HAM1*, *LIA1*, YJR071W, *NPA3*, *OPI3*, *MOG1*, *HOC1*	180
YGPM18p06	433497–443070	XII	*SMD3*, *PEP3*, YLR149C, YLR149C-A, *STM1*	180

[a] Jones et al. 2008; Thermo Scientific YSC4613, Waltham, MA, USA

[b] Nucleotide positions of the contig end sequences

[c] *S. cerevisiae* chromosome

[d] S288c *leu2Δ*/pGP564 (empty vector control) grew poorly or failed to grow at 140 mM acetic acid

monitoring A_{600} values as done here cannot distinguish these two effects, survival of treated cells was determined directly by plating on YNB+2 % glu. S288c *leu2Δ*/pGP564 and S288c *leu2Δ*/pGP564-*PEP3* sampled after a 1.5-h exposure to acetic acid exhibited 96±7 vs 97+8 % survival (140 mM) and 98±6 vs 98±4 % survival (160 mM), respectively. Control cells not exposed to acetic acid but plated after the same 1.5-h exposure exhibited limited growth as expected: 123±12 vs 140±5 % survival for S288c *leu2Δ*/pGP564 and S288c *leu2Δ*/pGP564-*PEP3*, respectively. While these results suggest that the prolonged lag phase of the acetic acid-exposed wild-type strain simply reflects the time needed to overcome acetic acid-induced growth inhibition, it is possible that incubation for longer than 1.5 h could have induced cell death. Because the strain transformed with pGPM18p06 not only had a reduced lag phase, but an increased growth rate, we presumed that an additional overexpressed gene on the pGPM18p06 contig played a protective role.

Because *STM1* was also on the pGPM18p06 contig—but not on others in the library—and had previously been implicated in protecting ribosomes from nutritional starvation-induced degradation (Van Dyke et al. 2006, 2013), we cloned *STM1* into pGP564 and constructed S288c *leu2Δ*/pGP564-*STM1* to evaluate its individual contribution to overcoming acetic acid-induced stress. In the absence of acetic acid, the lag phase of S288c *leu2Δ*/pGP564-*STM1* was about 70 % longer than that of the empty vector control strain and its growth rate was about 12 % slower. In the presence of 140 mM acetic acid, however, its lag phase was about 4 h, the same as for S288c *leu2Δ*/pGP564-*PEP3*, compared to 16.5 h for the empty vector control. Further, the growth rate of S288c *leu2Δ*/pGP564-*STM1* was about 40 % faster than that of the empty vector control, 35 % faster than that of S288c *leu2Δ*/pGP564-*PEP3*, and the same as the strain carrying the original contig, S288c *leu2Δ*/pGP564-pGPM18p06. At 160 mM acetic acid, its growth rate was twice as fast as that of the empty vector control and that of S288c *leu2Δ*/pGP564-*PEP3* and 25 % faster than that of S288c *leu2Δ*/pGP564-pGPM18p06. We conclude that both *PEP3* and *STM1* play major roles in reducing lag phase in acetic acid-stressed cells, but that overexpression of *STM1*, and not *PEP3*, increases growth rate.

PEP3-overexpressing cells are larger and more granular than wild-type cells

Under the light microscope, cells overexpressing *PEP3* were observed to be larger than wild-type cells (data not shown). To obtain a more accurate estimate, flow cytometry was used to measure both cell size and granularity (a measure of organelle content) in both strains. The *PEP3*-overexpression mutant was found to be 2-fold larger (409 vs 199 arbitrary units proportional to cell diameter) and to have greater granularity (225 vs 101 arbitrary units) than wild-type cells, consistent with an increased number of vacuoles (Fig. 1). *PEP3* overexpression was previously reported to increase cell size (Arlt et al. 2011).

PEP3-overexpressing cells have more fragmented vacuoles than wild-type cells

Based on the known role that *PEP3* plays in vacuole biogenesis and the increased granularity of the overexpression mutant, cells were stained with a vacuolar membrane-specific dye FM4-64 in order to test for the possibility of increased vacuole content. Stained cells were then observed by confocal microscopy and by flow cytometry. Wild-type cells exhibited normal vacuolar morphology with 1 to 3 vacuoles per cell while the overexpression mutant was found to have four or more vacuoles per cell (Fig. 2). Furthermore, as the number of the vacuolar structures

Table 3 Growth rate and lag phase duration in aerobic shake flask cultures

| Acetic acid treatment	Strain S288c leu2Δ/	lag (h)	μ (h^{-1})
No acid	pGP564	1.27±0.06[a]	0.34±0.00[a]
	pGP564-YGPM18p06	1.33±0.06[a]	0.36±0.00[b]
	pGP564-PEP3	1.27±0.06[a]	0.39±0.00[c]
	pGP564-STM1	2.17±0.32[b]	0.38±0.02[bcd]
	pGP564-PEP5	1.64±0.04[c]	0.38±0.00[d]
140 mM	pGP564	16.47±0.47[a]	0.19±0.01[a]
	pGP564-YGPM18p06	5.20±0.35[b]	0.25±0.01[b]
	pGP564-PEP3	3.97±0.59[c]	0.20±0.03[a]
	pGP564-STM1	3.73±0.21[c]	0.27±0.00[b]
	pGP564-PEP5	6.14±0.29[d]	0.15±0.02[a]
160 mM	pGP564	16.5±0.56[a]	0.12±0.00[a]
	pGP564-YGPM18p06	5.37±0.06[b]	0.20±0.01[b]
	pGP564-PEP3	6.23±0.25[c]	0.12±0.00[a]
	pGP564-STM1	5.20±0.26[b]	0.25±0.01[c]
	pGP564-PEP5	18.64±2.39[a]	0.18±0.00[d]

Dissimilar superscripts for lag or μ values within a treatment (0, 140, or 160 mM acetic acid) indicate statistically significant differences ($p<0.05$)

increased, the size of the individual vacuoles decreased. Our observations are consistent with earlier studies that reported that overexpression of *PEP3* resulted in more fragmented vacuoles (Arlt et al. 2011). Overexpression of another CORVET complex component Vps3 has also been reported to result in a similar change in vacuolar morphology (Peplowska et al. 2007).

FM4-64 fluorescence intensity was quantified by flow cytometry. This analysis confirmed similar autofluorescence (Smith

Fig. 1 Flow cytometric analysis of S288c leu2Δ/pGP564 (*red*) and S288c leu2Δ/pGP564-PEP3 (*blue*) cells (*n*=200,000)

et al. 2013) of the wild-type and *PEP3*-overexpression strains, but indicated greater FM4-64 fluorescence intensity in the *PEP3*-overexpression strain, 390 vs 108 arbitrary units (Fig. 3). Although the *PEP3*-overexpression strain was found to be about 2-fold larger than wild-type cells, the FM4-64 fluorescence intensity was 3.6-fold higher corresponding to more vacuolar membrane per cell in the *PEP3*-overexpression strain.

We next examined vacuolar morphology in the *PEP3*-overexpression and wild-type strains as a function of exposure to 80 mM acetic acid, a concentration that caused no apparent growth defect. By confocal microscopy, vacuoles in the wild-type strain stained with FM4-64 in the presence of acetic acid were fragmented relative to the absence of acid (Fig. 4). In contrast, no difference was observed in vacuolar morphology in the *PEP3*-overexpression mutant in the presence or absence of acetic acid (Fig. 4). An estimate of vacuolar surface-to-volume ratio was made to determine whether the change in morphology in the *PEP3*-overexpression strain and in the wild-type control exposed to 80 mM acetic acid resulted in an increase in this parameter as previously observed for osmotically shocked cells (Zieger and Mayer 2012). As shown in Table 4, an increase was observed in the *PEP3*-overexpression strain relative to the wild-type strain both in the presence and absence of added acetic acid and in acetic acid-treated wild-type cells relative to untreated wild-type cells. No significant difference in vacuolar surface-to-volume ratio was observed between acid-treated and untreated *PEP3*-overexpressing cells. Similar vacuolar fragmentation has been observed in *S. cerevisiae* exposed to lactic and hydrochloric acids (Suzuki et al. 2012). Vacuolar fragmentation has also been
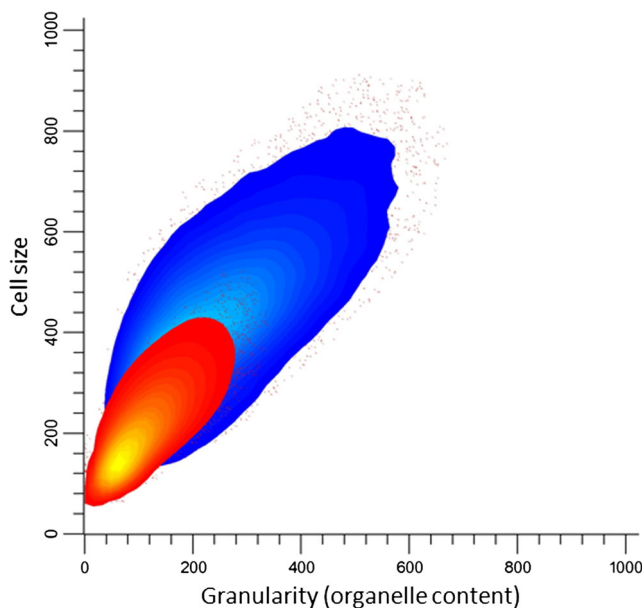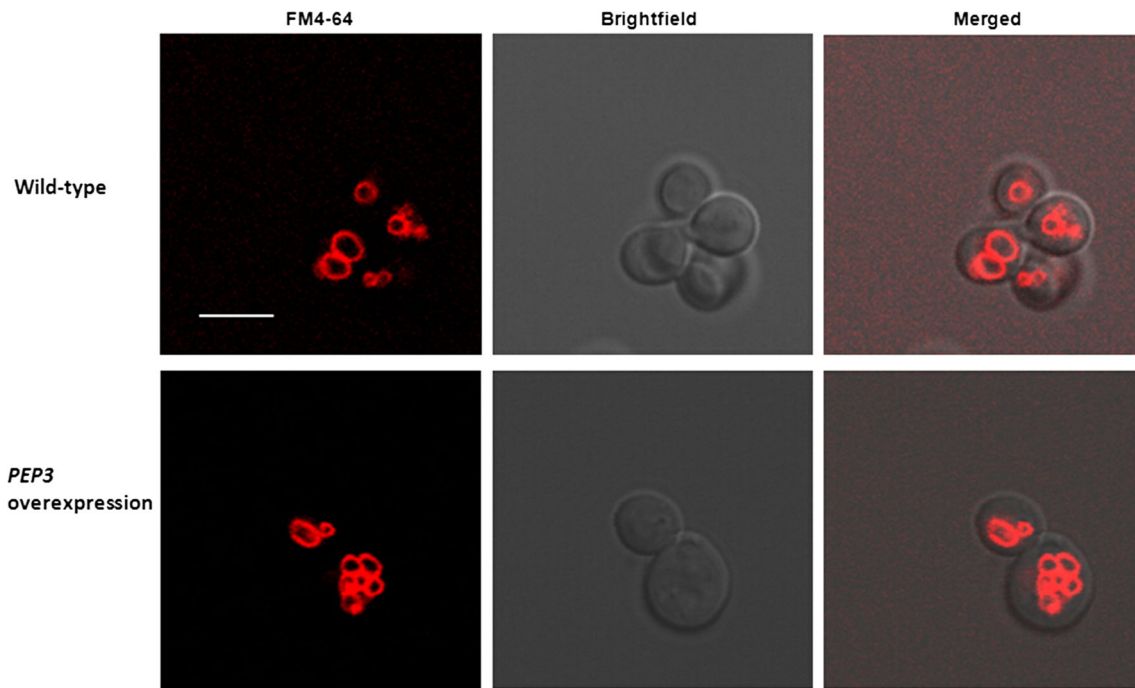
Fig. 2 Confocal microscopy of FM4-64-stained S288c *leu2Δ*/pGP564 (*upper panel*) and S288c *leu2Δ*/pGP564-*PEP3* (*lower panel*). Representative images are shown; >25 cells per strain were observed. *Scale bar*, 5 μm

reported in calcium- and sodium-stressed cells presumably to increase uptake of these ions by increasing vacuolar surface-to-volume ratio (Kellermayer et al. 2003). Vacuolar fragmentation has also been proposed to alter vacuolar membrane tension and
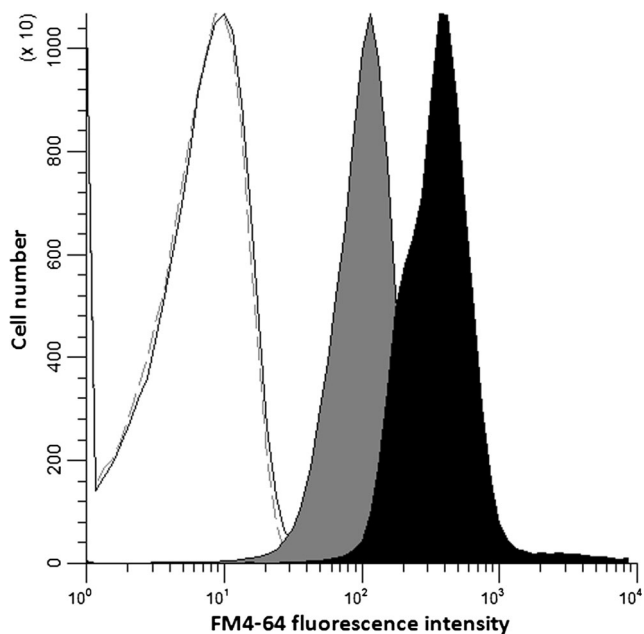
Fig. 3 Flow cytometric analysis of FM4-64-stained S288c *leu2Δ*/pGP564 (*solid grey*) and S288c *leu2Δ*/pGP564-*PEP3* (*solid black*). Autofluorescence of the two strains was the same (*overlapping grey and black lines*). FM4-64 median fluorescence intensity in arbitrary units was 108.14 (S288c *leu2Δ*/pGP564) vs 389.84 (S288c *leu2Δ*/pGP564-*PEP3*), *n*=200,000

thereby activity of membrane proteins (Zieger and Mayer 2012). More generally, a number of environmental and intrinsic factors have been proposed to control a dynamic balance between vacuolar membrane fusion and fission events during growth, including transmission of vacuoles from mother to daughter cells (Weisman 2003; Michaillat et al. 2012). Acid stress appears to shift the balance in the direction of fission.

In order to determine whether overexpression of another component shared by both the HOPS and CORVET complexes could also improve growth response in acetic acid-stressed cells, we cloned *PEP5* whose deletion had previously been found to result in increased sensitivity to acetic (Kawahata et al. 2006) and lactic (Suzuki et al. 2012) acids. As shown in Table 3, in the absence of acetic acid, overexpression of *PEP5* was found to increase lag phase by 30 % relative to both the empty vector control and to S288c *leu2Δ*/pGP564-*PEP3*, while growth rate increased 12 and 2 % relative to the empty vector control and S288c *leu2Δ*/pGP564-*PEP3*, respectively. In the presence of 140 mM acetic acid, *PEP5* overexpression reduced lag phase to 6 h from 16.5 h for the empty vector control, whereas overexpression of *PEP3* reduced lag phase to 4 h. Growth rates were the same for S288c *leu2Δ*/pGP564-*PEP5*, the empty vector control, and S288c *leu2Δ*/pGP564-*PEP3*. In the presence of 160 mM acetic acid, the lag phase of the *PEP5*-overexpression strain was the same as that of the empty vector control but far less than that of S288c *leu2Δ*/pGP564-*PEP3*, 6 h. The growth rate of S288c *leu2Δ*/pGP564-*PEP5* was 50 % faster than that of either the empty vector control or S288c *leu2Δ*/pGP564-
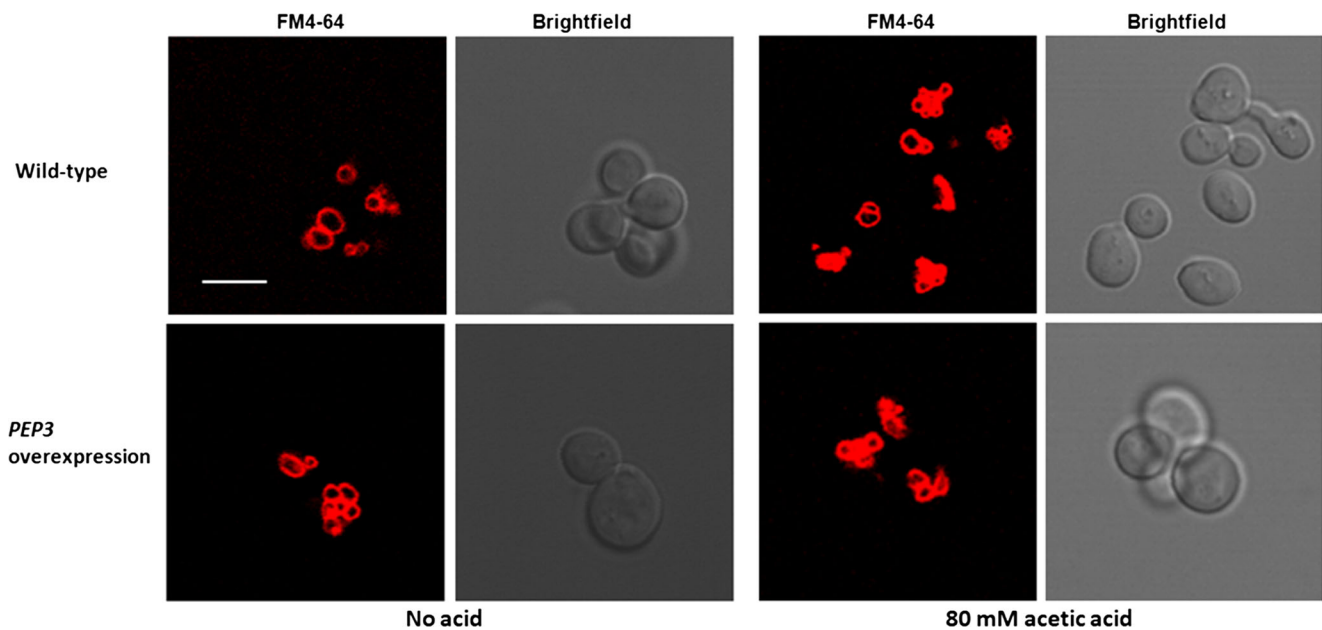
Fig. 4 Representative confocal images of FM4-64-stained S288c *leu2Δ*/pGP564 (*upper panel*) and S288c *leu2Δ*/pGP564-*PEP3* (*lower panel*) in the presence and absence of 80 mM acetic acid; >25 cells were viewed per strain-treatment combination. *Scale bar*, 5 μm

PEP3. It appears that overexpression of *PEP5* is also beneficial in acetic acid-stressed cells. It reduced lag phase duration at 140 mM acetic acid almost as well as overexpression of *PEP3*, while at 160 mM acetic acid, it did not decrease lag, but increased growth rate, unlike *PEP3* overexpression.

PEP3 overexpression results in more acidic vacuoles in the presence of 80 mM acetic acid

Vacuolar acidification based on quinacrine staining was compared between the *PEP3*-overexpression mutant and wild-type strain grown in the presence or absence of acetic acid. Quinacrine is a weakly basic dye that accumulates in acidic compartments in response to proton gradients and is routinely used to assess the state of vacuolar acidification in yeast

(Hughes and Gottschling 2012). Cells were incubated in the presence or absence of 80 mM acetic acid. Cells from both strains grown in the absence of acetic acid displayed strongly localized vacuolar fluorescence indicative of a normal acidic vacuole (Fig. 5a). *PEP3*-overexpressing cells were found to have more intensely fluorescent vacuoles than wild-type cells regardless of acid exposure based on fluorometry (Fig. 5b).

Because the fluorescence intensity of quinacrine increases as pH decreases, the greater fluorescence per cell could be due to a lower vacuolar pH but also to more vacuoles/cell in the *PEP3*-overexpression strain. To assess the former possibility, we measured vacuolar pH in both mutant and wild-type cells using a vacuolar-specific pH-sensitive fluorescent probe (acetoxymethyl ester of the fluorescein-based probe BCECF), which has previously been used to measure vacuolar

Table 4 Estimate of vacuolar surface-to-volume ratio

Strain, treatment	Diameter (μ)	Surface/volume (μ^{-1})	p value for indicated comparison of surface/volume ratio	p value for indicated comparison of surface/volume ratio
#1 S288c *leu2Δ*/pGP564 No acid	1.73	3.47	<0.001 #1 vs #2	<0.01 #1 vs #3
#2 S288c *leu2Δ*/pGP564-*PEP3* No acid	1.25	4.79		
#3 S288c *leu2Δ*/pGP564 80 mM acetic acid	1.48	4.05	<0.05 #1 vs #4	Not significant #2 vs #4
#4 S288c *leu2Δ*/pGP564-*PEP3* 80 mM acetic acid	1.34	4.49		

[a] Measurements were made on no fewer than 16 FM4-64-stained vacuoles per strain-treatment combination as described (Zieger and Mayer 2012)

A

B
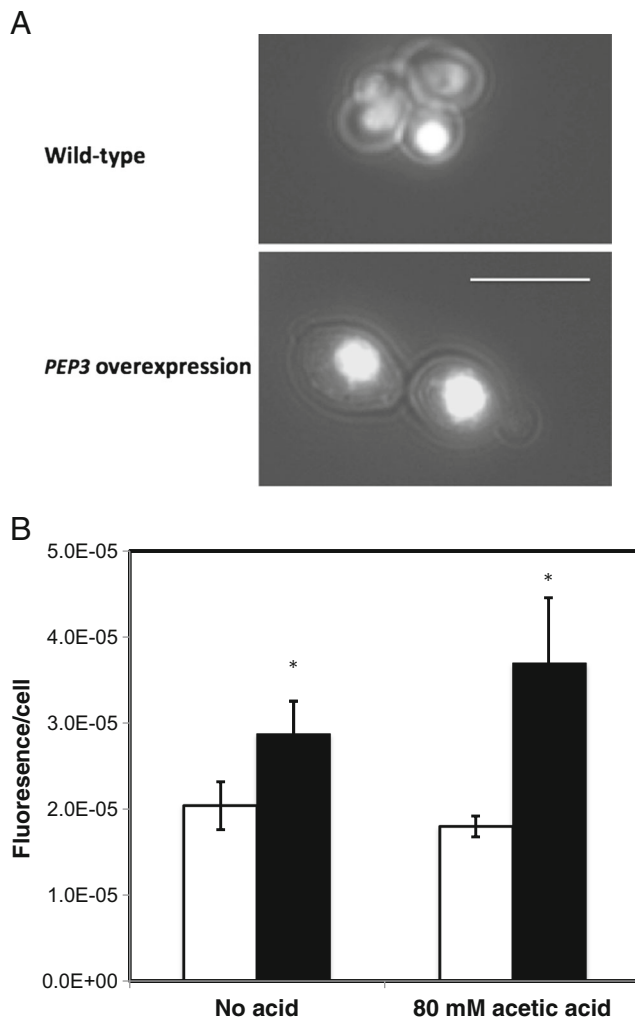
Fig. 5 Quinacrine staining by fluorescence microscopy. **a** Vacuolar localization of quinacrine in S288c *leu2*Δ/pGP564 (*upper panel*) and S288c *leu2*Δ/pGP564-*PEP3* (*lower panel*). *Scale bar*, 5 μm. **b** Fluorescence intensity of quinacrine-stained S288c *leu2*Δ/pGP564 (*white bar*) and S288c *leu2*Δ/pGP564-*PEP3* (*black bar*). Data are means±standard deviations (*n*=3). Fluorescence intensity (arbitrary units) was quantified using a fluorometer and normalized to cell number. The *asterisk* indicates a significant difference in fluorescence intensity between the *PEP3* overexpression and the wild type strains, *p*<0.05

pH in yeast (Diakov et al. 2013; Plant et al. 1999; Ali et al. 2004). Wild-type and *PEP3*-overexpressing cells grown to log phase in the presence or absence of 80 mM acetic acid were stained with BCECF-AM and vacuolar pH was then measured. Vacuolar localization of the dye by fluorescence microscopy was confirmed in both strains in the presence and absence of acetic acid (data not shown). The vacuolar pH of the wild-type strain and the *PEP3*-overexpression mutant in the absence of acetic acid was not significantly different (5.62±0.19 vs 5.90±0.11, respectively). These values are similar to those measured in wild-type cells by other techniques (Padilla-López and Pearce 2006; Preston et al. 1989; Martínez-Muñoz and Kane 2008). A slight but insignificant increase in vacuolar pH was observed in the

PEP3-overexpression mutant when cells were grown in the presence of 80 mM acetic acid, reaching a value of 6.14±0.18. However, in wild-type cells, the vacuolar pH increased significantly to 6.35±0.09 (*p*<0.05), similar to previous observations of *vma2*Δ and *vma3*Δ mutants which lack V-ATPase activity (Martínez-Muñoz and Kane 2008). Our results suggest a deficiency in vacuolar acidification in acetic acid-stressed wild-type cells, but not in the *PEP3*-overexpression mutant.

V-ATPase activity is higher in *PEP3*-overexpressing cells

V-ATPase is essential for regulating vacuolar pH (Martínez-Muñoz and Kane 2008). Therefore, one explanation for the increased resistance of the *PEP3*-overexpression mutant to acetic acid is that it has greater V-ATPase activity than wild-type cells and, hence, a greater ability to sequester protons in the vacuole. V-ATPase activity is essential in yeast when cells grow on glucose at pH 7.5 (Nelson and Nelson 1990) and in cells growing on the non-fermentable substrate glycerol (Ohya et al. 1991). One of the defining phenotypes of *vma*Δ mutants, which lack V-ATPase activity, is their inability to grow at high pH or to use glycerol as a sole carbon source (Nelson and Nelson 1990; Ohya et al. 1991). Therefore, two indirect assays were performed using the V-ATPase-specific inhibitor, concanamycin A, to assess relative V-ATPase activity in both strains in vivo. We speculated that if V-ATPase activity were higher in the *PEP3*-overexpression mutant than in wild-type cells, the mutant would be better able to grow at pH 7.5 and better able to grow on glycerol than the wild-type strain when exposed to the same concentration of inhibitor. Relative growth of each strain was calculated based on growth in the presence vs absence of inhibitor after 24 h. Figure 6 shows that growth of the *PEP3*-overexpression mutant was better in the presence of the same amount of concanamycin A. When grown in YEPG-5 in the absence of concanamycin A, A_{600} values were about 0.11 in both strains. However, the A_{600} value decreased to 0.033 for the wild-type strain compared to 0.054 for the *PEP3*-overexpression strain in the presence of 2 μM concanamycin. The corresponding relative growth was 49 % for the *PEP3*-overexpression strain compared to 30 % for wild-type cells (Fig. 6a). Larger differences were observed when cells were grown in YEPD-7.5 supplemented with 1 μM concanamycin A. In the absence of concanamycin A, A_{600} values were 5.28 for the wild-type parent and 2.36 for the *PEP3*-overexpression strain. However, in the presence of 1 μM concanamycin A, the A_{600} value decreased to 0.15 and 0.71 for the wild-type and *PEP3*-overexpression strains, respectively. The corresponding relative growth of the *PEP3*-overexpression strain was 30 % compared to only 3 % for the wild-type parent (Fig. 6b). By this indirect measure, *PEP3* overexpression appears to increase V-ATPase activity.
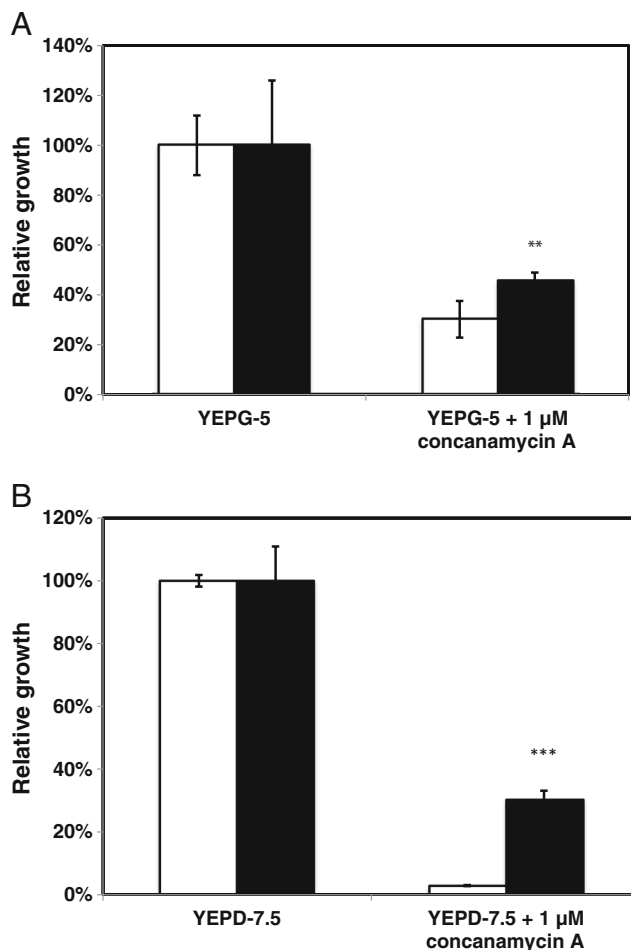
Fig. 6 Effect of *PEP3* overexpression on V-ATPase activity. **a** S288c *leu2Δ*/pGP564-*PEP3* (*black bar*) exhibited better relative growth in the presence of the V-ATPase inhibitor concanamycin A than S288c *leu2Δ*/pGP564 (*white bar*) in YEPG-5 and in **b** YEPD-7.5. Data are means± standard deviations (*n*=3). *Asterisks* indicate a significant difference between the strains, **$p<0.01$, ***$p<0.001$. The relative growth assay is defined in "Materials and methods" (indirect measurement of V-ATPase activity)

Effect of *PEP3* overexpression on protein level and expression of V-ATPase

In order to determine if the apparent greater V-ATPase activity was due to an increased level of V-ATPase enzyme in the *PEP3*-overexpression strain, we compared the amount of one subunit, Vma2 (60 kDa), as a marker for overall V-ATPase abundance in whole protein extracts from wild-type and the *PEP3*-overexpression strain by western blotting. As shown in Fig. S1 of the Supplementary Material, the level of Vma2 appeared to be higher in the *PEP3*-overexpression strain compared to a GADPH loading control. Immunoblot analysis indicated a significantly higher signal for the overexpression strain, about 30 % greater than for the wild-type strain. We next assessed expression levels of *VMA2* in the

wild-type and *PEP3*-overexpression strain. RT-qPCR analysis showed that while *PEP3* expression was 60-fold higher in the overexpression strain, an insignificant increase in *VMA2* expression was observed between the two tested strains, a 0.7-fold change. Expression of a second gene encoding a V-ATPase component, Vph1, was also measured by RT-qPCR. No significant difference was observed in expression levels between the wild-type and *PEP3*-overexpressing strain (0.5-fold change). We conclude that *PEP3* overexpression does not regulate V-ATPase at the transcriptional level.

Discussion

The use of the 2 μ-based overexpression library to screen for acetic acid-resistant mutants offered an important advantage over current deletion libraries. The plasmid carries *LEU2* which allowed use of a strain that had a sole auxotrophic marker—*leu2*. Because transformants acquired *LEU2*, they were not dependent on provision of leucine in the medium. We and others have previously shown that the ability of acetic acid-stressed cells to take up nutrients is compromised and that mutations that confer acetic acid resistance in an auxotrophic background tend to select for defects in endocytosis and response to nutritional starvation and are unlikely to confer similar resistance in a prototrophic background (Bauer et al. 2003; Hueso et al. 2012; Ding et al. 2013). Nonetheless, all cells must take up essential nutrients that they cannot make, e.g., sulfate, phosphate, and hence, while avoidance of auxotrophic mutations is helpful, it does not completely eliminate the deleterious effect of acetic acid on nutrient uptake.

Because *PEP3* is involved in vacuolar biogenesis and can plausibly impinge upon the endocytosis or vacuolar degradation of plasma membrane transporters, we tested whether its overexpression affected nutrient uptake in acetic acid-stressed cells. For both histidine and lysine uptake, overexpression of *PEP3* did not ameliorate the effect of acetic acid on uptake (Table S2 in the Supplementary Material).

While it is coincidental that the only intact copies of *PEP3* and *STM1* in the overexpression library were isolated on the same contig—pGP564-YGM18p06—assessment of growth rate and lag phase duration was a helpful step in distinguishing their individual contributions to acetic acid "resistance." Our finding that *STM1* overexpression both increased growth rate and reduced lag phase duration in acetic acid-stressed cells is consistent with previous work that showed a role for *STM1* in protecting a subset of ribosomes from degradation during autophagy (Van Dyke et al. 2006, 2013). We speculate that such cells are more likely to begin growth sooner and to grow faster once they have recovered from the initial acetic acid shock than cells whose ribosomes have been largely degraded. In contrast, *PEP3* overexpression decreased lag phase duration but had no affect on growth rate. The vacuolar fragmentation

phenotype associated with *PEP3* overexpression has also been observed in wild-type cells upon exposure to acid stress alone (acetic acid in the present study; lactic and hydrochloric acid-induced in previous work [Suzuki et al. 2012]) similar to the response to osmotic shock (Zieger and Mayer 2012; Kellermayer et al. 2003). At sublethal concentrations of the acid or osmolyte, this response is presumed to be protective as it results in greater vacuolar surface area and, thus, greater sequestration potential. Because *PEP3*-overexpressing cells have more fragmented vacuoles than wild-type cells even in the absence of acid, we speculate that they are in a sense preconditioned for acid stress and, hence, exhibit greater acid resistance.

The question of how overexpression of *PEP3* that encodes a single member of a tethering complex involved in vacuole biogenesis could cause vacuolar fragmentation is unclear. Based on the model proposed by Michaillat et al. (2012) which posits that a number of environmental and genetic factors can shift the balance of vacuole fusion and fission events, and the observation that overexpression of a single member of a protein complex is generally disruptive of complex function (Papp et al. 2003), it is possible that overexpression of *PEP3* may shift the balance towards fission events by interfering with the HOPS complex-mediated fusion reaction. A previous genome-wide screen of a different overexpression library for vacuole morphology variants detected *PEP3*, *VPS39*—encoding another HOPS component and *VPS3*, encoding a CORVET component—but not other genes encoding additional components of these complexes. Interestingly, a new function for Vps39 in mediating contact between mitochondria and vacuoles was recently revealed by overexpression of *VPS39* (Hönscher et al. 2014). By analogy, it is possible that *PEP3* alone or in concert with other non-HOPS component(s) is able to stimulate vacuolar fission.

While *PEP3*, *PEP5*, and *STM1* are potential targets for modification in industrial strains used for cellulosic ethanol production, the possibility that overexpression could lead to undesirable phenotypes that might compromise other valued traits must also be evaluated. The additional candidate genes identified in the present screen (Table 2) but which were not subjected to analysis represent new potential targets worthy of consideration.

References

Ali R, Brett CL, Mukherjee S, Rao R (2004) Inhibition of sodium/proton exchange by a Rab-GTPase-activating protein regulates endosomal traffic in yeast. J Biol Chem 279:4498–4506

Arlt H, Perz A, Ungermann C (2011) An overexpression screen in *Saccharomyces cerevisiae* identifies novel genes that affect endocytic protein trafficking. Traffic 12:1592–1603

Bauer BE, Rossington D, Mollapour M, Mamnun Y, Kuchler K, Piper PW (2003) Weak organic acid stress inhibits aromatic amino acid uptake by yeast, causing a strong influence of amino acid auxotrophies on the phenotypes of membrane transporter mutants Eur. J Biochem 270:3189–3195

Balderhaar HJ, Ungermann C (2013) CORVET and HOPS tethering complexes–coordinators of endosome and lysosome fusion. J Cell Sci 126:1307–1316

Bradford MM (1976) A rapid and sensitive method for the quantitation of microgram quantities of protein utilizing the principle of protein-dye binding. Anal Biochem 72:248–254

Coonrod EM, Graham LA, Carpp LN, Carr TM, Stirrat L, Bowers K, Stevens TH (2013) Homotypic vacuole fusion in yeast requires organelle acidification and not the V-ATPase membrane domain. Dev Cell 27:462–468

Diakov TT, Tarsio M, Kane PM (2013) Measurement of vacuolar and cytosolic pH in vivo in yeast cell suspensions. J Vis Exp 74, e50261. doi:10.3791/50261

Ding J, Bierma J, Smith MR, Poliner E, Wolfe C, Hadduck AN, Bakalinsky AT (2013) Acetic acid inhibits nutrient uptake in *Saccharomyces cerevisiae*: auxotrophy confounds the use of yeast deletion libraries for strain improvement. Appl Microbiol Biotechnol 97:7405–7416

Eraso P, Gancedo C (1987) Activation of yeast plasma membrane ATPase by acid pH during growth. FEBS Lett 224:187–192

Gietz RD, Schiestl RH, Willems AR, Woods RA (1995) Studies on the transformation of intact yeast cells by the LiAc/SS-DNA/PEG procedure. Yeast 11:355–360

Harding TM, Morano KA, Scott SV, Klionsky DJ (1995) Isolation and characterization of yeast mutants in the cytoplasm to vacuole protein targeting pathway. J Cell Biol 131:591–602

Hönscher C, Mari M, Auffarth K, Bohnert M, Griffith J, Geerts W, van der Laan M, Cabrera M, Reggiori F, Ungermann C (2014) Cellular metabolism regulates contact sites between vacuoles and mitochondria. Dev Cell 30:86–94

Hueso G, Aparicio-Sanchis R, Montesinos C, Lorenz S, Murguía JR, Serrano R (2012) A novel role for protein kinase Gcn2 in yeast tolerance to intracellular acid stress. Biochem J 441:255–264

Hughes AL, Gottschling DE (2012) An early age increase in vacuolar pH limits mitochondrial function and lifespan in yeast. Nature 492:261–265

Jones GM, Stalker J, Humphray S, West A, Cox T, Rogers J, Prelich G (2008) A systematic library for comprehensive overexpression screens in *Saccharomyces cerevisiae*. Nat Methods 5:239–241

Kawahata M, Masaki K, Fujii T, Lefuji H (2006) Yeast genes involved in response to lactic acid and acetic acid: acidic conditions caused by the organic acids in *Saccharomyces cerevisiae* cultures induce expression of intracellular metal metabolism genes regulated by Aft1p. FEMS Yeast Res 6:924–936

Kellermayer R, Aiello DP, Miseta A, Bedwell DM (2003) Extracellular Ca^{2+} sensing contributes to excess Ca^{2+} accumulation and vacuolar fragmentation in a pmr1Δ mutant of *S. cerevisiae*. J Cell Sci 116:1637–1646

Lawrence CL, Botting CH, Antrobus R, Coote PJ (2004) Evidence of a new role for the high-osmolarity glycerol mitogen-activated protein kinase pathway in yeast: regulating adaptation to citric acid stress. Mol Cell Biol 24:3307–3323

Li SC, Kane PM (2009) The yeast lysosome-like vacuole: endpoint and crossroads. Biochim Biophys Acta 1793:650–663

Martínez-Muñoz GA, Kane PM (2008) Vacuolar and plasma membrane proton pumps collaborate to achieve cytosolic pH homeostasis in yeast. J Biol Chem 283:20309–20319

Michaillat L, Baars TL, Mayer A (2012) Cell-free reconstitution of vacuole membrane fragmentation reveals regulation of vacuole size and number by TORC1. Mol Biol Cell 23:881–895

Mira NP, Teixeira MC, Sá-Correia I (2010) Adaptive response and tolerance to weak acids in *Saccharomyces cerevisiae*: a genome-wide view. OMICS 14:525–540

Mollapour M, Piper PW (2007) Hog1 mitogen-activated protein kinase phosphorylation targets the yeast Fps1 aquaglyceroporin for endocytosis, thereby rendering cells resistant to acetic acid. Mol Cell Biol 27:6446–6456

Nakamura N, Hirata A, Ohsumi Y, Wada Y (1997) Vam2/Vps41p and Vam6/Vps39p are components of a protein complex on the vacuolar membranes and involved in the vacuolar assembly in the yeast *Saccharomyces cerevisiae*. J Biol Chem 272:11344–11349

Nelson H, Nelson N (1990) Disruption of genes encoding subunits of yeast vacuolar H($^+$)-ATPase causes conditional lethality. Proc Natl Acad Sci 87:3503–3507

Nichols BJ, Ungermann C, Pelham HR, Wickner WT, Haas A (1997) Homotypic vacuolar fusion mediated by t- and v-SNAREs. Nature 387:199–202

Ohya Y, Umemoto N, Tanida I, Ohta A, Iida H, Anraku Y (1991) Calcium-sensitive cls mutants of *Saccharomyces cerevisiae* showing a Pet$^-$ phenotype are ascribable to defects of vacuolar membrane H$^+$-ATPase activity. J Biol Chem 266:13971–13977

Padilla-López S, Pearce DA (2006) *Saccharomyces cerevisiae* lacking Btn1p modulate vacuolar ATPase activity to regulate pH imbalance in the vacuole. J Biol Chem 281:10273–10280

Palmqvist E, Hahn-Hägerdal B (2000) Fermentation of lignocellulosic hydrolysates. I: inhibition and detoxification. Bioresour Technol 74:17–24

Papp B, Pál C, Hurst LD (2003) Dosage sensitivity and the evolution of gene families in yeast. Nature 424:194–197

Peplowska K, Markgraf DF, Ostrowicz CW, Bange G, Ungermann C (2007) The CORVET tethering complex interacts with the yeast Rab5 homolog Vps21 and is involved in endo-lysosomal biogenesis. Dev Cell 1:739–750

Pfaffl MW (2001) A new mathematical model for relative quantification in real-time RT-PCR. Nucleic Acids Res 29:e45

Plant PJ, Manolson MF, Grinstein S, Demaurex N (1999) Alternative mechanisms of vacuolar acidification in H$^+$-ATPase-deficient yeast. J Biol Chem 274:37270–37279

Preston RA, Murphy RF, Jones EW (1989) Assay of vacuolar pH in yeast and identification of acidification-defective mutants. Proc Natl Acad Sci 86:7027–7031

Price A, Seals D, Wickner W, Ungermann C (2000) The docking stage of yeast vacuole fusion requires the transfer of proteins from a Cis-snare complex to a Rab/Ypt protein. J Cell Biol 148:1231–1238

Schauer A, Knauer H, Ruckenstuhl C, Fussi H, Durchschlag M, Potocnik U, Fröhlich KU (2009) Vacuolar functions determine the mode of cell death. Biochim Biophys Acta 1793:540–545

Schumacher K, Krebs M (2010) The V-ATPase: small cargo, large effects. Curr Opin Plant Biol 13:724–730

Smith MR, Boenzli MG, Hindagolla V, Ding J, Miller JM, Hutchison JE, Bakalinsky AT (2013) Identification of gold nanoparticle-resistant mutants of *Saccharomyces cerevisiae* suggests a role for respiratory metabolism in mediating toxicity. Appl Environ Microbiol 79: 728–733

Sobanski MA, Dickinson JR (1995) A simple method for the direct extraction of plasmid DNA from yeast. Biotechnol Tech 9:225–230

Suzuki T, Sugiyama M, Wakazono K, Kaneko Y, Harashima S (2012) Lactic-acid stress causes vacuolar fragmentation and impairs intracellular amino-acid homeostasis in *Saccharomyces cerevisiae*. J Biosci Bioeng 113:421–430

Swinnen S, Fernández Niño M, González-Ramos D, van Maris AJA, Nevoigt E (2014) The fraction of cells that resume growth after acetic acid addition is a strain-dependent parameter of acetic acid tolerance in *Saccharomyces cerevisiae*. FEMS Yeast Res 14:642–653

Tal R, Winter G, Ecker N, Klionsky DJ, Abeliovich H (2007) Aup1p, a yeast mitochondrial protein phosphatase homolog, is required for efficient stationary phase mitophagy and cell survival. J Biol Chem 282:5617–5624

Van Dyke N, Baby J, Van Dyke MW (2006) *STM1*p, a ribosome-associated protein, is important for protein synthesis in *Saccharomyces cerevisiae* under nutritional stress conditions. J Mol Biol 358:1023–1031

Van Dyke N, Chanchorn E, Van Dyke MW (2013) The *Saccharomyces cerevisiae* protein *STM1*p facilitates ribosome preservation during quiesence. Biochem Biophys Res Commun 430:745–750

Weisman LS (2003) Yeast vacuole inheritance and dynamics. Annu Rev Genet 37:435–460

Wickner W (2010) Membrane fusion: five lipids, four SNAREs, three chaperones, two nucleotides, and a Rab, all dancing in a ring on yeast vacuoles. Annu Rev Cell Dev Biol 26:115–136

Xu X, Wightman JD, Geller BL, Avram D, Bakalinsky AT (1994) Isolation and characterization of sulfite mutants of *Saccharomyces cerevisiae*. Curr Genet 25:488–496

Zieger M, Mayer A (2012) Yeast vacuoles fragment in an asymmetrical two-phase process with distinct protein requirements. Mol Biol Cell 23:3438–3449